Polyoxometalates

RESEARCH ARTICLE

Synthesis and characterization of lead(II)-containing heteropolytungstates, $[Pb^{II}(\alpha\text{-}XW_{11}O_{39})]^{6-}$ (X = Si, Ge)

Lakita Khidtta, Nickolet Ncube, Anupam Sarkar, Ananthu Rajan, Arnav A. Gaikwad, and Ulrich Kortz

School of Science, Constructor University, Campus Ring 1, 28759 Bremen, Germany

Received: 1 August 2026; **Revised:** 29 October 2026; **Accepted:** 10 November 2026

Address correspondence to Anupam Sarkar, anusarkar@constructor.university; Ulrich Kortz, ukortz@constructor.university

Cite This: *Polyoxometalates*, 2027, *6*, 9140176

Read Online

ABSTRACT: We report on the synthesis and structural characterization of two lead(II)-containing heteropolytungstates. The two polyanions $[Pb^{II}(\alpha\text{-}XW_{11}O_{39})]^{6-}$ (X = Si, Ge) are of the Keggin type and they were synthesized *via* a simple one-pot synthetic procedure in aqueous medium. The title polyanions comprise a Pb^{II} ion incorporated in the lacunary site of the monovacant Keggin ion $[\alpha\text{-}XW_{11}O_{39}]^{8-}$ (X = Si, Ge). In the solid state, individual polyanions are connected to a neighboring one via four Pb-O(W) linkages, resulting in a zigzag chain. Upon dissolution, free polyanions $[Pb^{II}(\alpha\text{-}XW_{11}O_{39})]^{6-}$ (X = Si, Ge) with *Cs* symmetry are present in solution, as demonstrated by ^{183}W NMR showing a 6-line spectrum. Both polyanions were further characterized in the solid state by single-crystal XRD, FT-IR, and thermogravimetric and elemental analyses.

KEYWORDS: polyoxometalates, lead, tungstosilicate, isostructural

Just Accepted

1 Introduction

Polyoxometalates (POMs) constitute a versatile class of discrete transition metal-oxo anions with remarkable structural and electronic diversity [1]. A particularly important feature of POMs is the formation of vacant (lacunary) species by the removal of one or more addenda atoms, allowing to incorporate one or more guest metal ions, mostly from the *d*-block [2]. The incorporation of main group metal ions is more rare, the most prominent example probably being Sn^{IV} or organo-Sn^{IV} [3-7]. As concerns the larger congener Pb, the high-valent Pb^{IV} is easily reduced to Pb^{II} at ambient conditions and in aqueous solution, and hence the question arises what POM-derivatives are known with such guest. The Pb^{II} ion has a large ionic radius, flexible coordination geometry, and a stereochemically active $6s^2$ lone pair, allowing it to adopt a range of coordination numbers [8,9]. Despite these features, Pb-containing POMs remain comparatively rare, and their development has progressed through only a small number of structurally or spectroscopically defined examples. We are not aware of a structurally well-defined Pb^{IV}-containing polyoxotungstate, but in 2019 a polyoxo-12-palladate(II) with a Pb^{IV} guest was reported [10].

As concerns Pb^{II}-containing classical POMs, in 1982 Tourné and co-workers reported $[Pb^{II}GaW_{11}O_{39}]^{7-}$, with a Pb^{II} ion incorporated in a monolacunary Keggin 11-tungstogallate(III) ion [11]. The Pb^{II} center is four-coordinate, with two short Pb-O bonds of 2.37 Å and two longer Pb-O bonds of 2.49 Å. A year later, the same group reported $[Pb^{II}PW_{11}O_{39}]^{5-}$ which was characterized in solution by two-dimensional ^{183}W NMR (COSY and 2D INADEQUATE) [12]. The crystal structure of this polyanion is still unknown but is presumably identical to $[Pb^{II}GaW_{11}O_{39}]^{7-}$. After these early lacunary Keggin examples, the next distinct lead-containing POM appeared in 2000, when Radkov and Beer reported an organolead derivative of the Nb-substituted Keggin anion, $[PW_{11}O_{39}NbO(PbMe_3)]^{3-}$ [13]. A further advance came in 2009, when Mizuno and co-workers reported the inorganic cryptand $[Pb(\gamma\text{-}SiW_{10}O_{32})_2(\mu\text{-}O)_4]^{6-}$, in which a Pb^{II} ion is encapsulated by two γ-Keggin-ions [14]. This compound demonstrated that Pb^{II} can also be stabilized in a highly coordinated, cavity-bound environment rather than occupying a simple monolacunary Keggin site.

Since 2016, the chemistry of Pb-containing POMs has expanded mainly through non-lacunary coordination polymers and hybrid materials. Sokolov and co-workers reported Pb^{II} complexes with plenary Keggin and Wells-Dawson ions, including $[Pb_2(\mu_2\text{-}DMF)_2(DMF)_8][SiW_{12}O_{40}]$ and a Dawson-based Pb-DMF coordination polymer, where Pb^{II} acts as an external linker rather than occupying a POM lacunary site [15]. In 2018, Pb^{II}-containing reduced molybdophosphate hybrids based on $\{P_4Mo_6\}$ units were reported [16], followed by a Pb^{II}_2-DMF-linked chain based on the Nb^{V}-substituted Keggin ion $[PW_{11}Nb^{V}O_{40}]^{4-}$ [17]. In 2019, Pb^{II}–DMF-modified Keggin compounds such as $[Pb^{II}(DMF)_7]_2[SiW_{12}O_{40}]$ and $[Pb^{II}(DMF)_4(H_2O)_2][Pb^{II}_2(\mu_2\text{-}DMF)_2(DMF)_8][PW_{12}O_{40}]_2$ were shown to display reversible photochromism [18]. The same year witnessed the emergence of $[Ln_6O_8]$-encapsulating polyplumbites $[Ln_6(OH)_8(H_{30}Pb_{18}^{II}O_{32})]^{12+}$ (Ln^{III} = Y, Sm, Eu, Gd, Tb, Dy, and Ho) and $\{[Ln_6(OH)_8(H_{32}Pb^{II}_{18}O_{32})]_{0.5}[Ln_6(OH)_8(H_2O)_6(H_{24}Pb^{II}_{12}O_{24})]_{0.5}\}^{12+}$ (Ln^{III} = Er, Tm) in which Pb forms polynuclear oxo-cages [19]. A reinvestigation of $[PW_{11}O_{39}Pb^{II}]^{5-}$ in 2021 by the Sokolov team

provided a rather complete characterization, including multinuclear NMR, HR-ESI-MS, XANES/EXAFS, DFT, cyclic voltammetry, and photoluminescence studies [20]. In 2023, a Pb^{II}-linked Dawson-type 18-molybdate $(Pb(DMF)_4)_3[P_2Mo_{18}O_{62}]_2$ was reported with photochromic and impedance response [21], and in 2025 α_2-$[P_2W_{17}O_{61}Pb^{II}]^{8-}$ was used as a labile monolacunary Wells–Dawson Pb^{II} precursor for the aqueous synthesis of PbS nanocrystals [22]. Overall, the known Pb–POM structures show that Pb^{II} can function as a lacunary-site occupant, encapsulated guest, external linker, organometallic graft, framework-forming addenda element, or precursor ion. These examples highlight the structural flexibility of Pb^{II} in POM chemistry and suggest its ability to adapt to diverse oxygen-donor environments and provide a strong basis for further development of Pb^{II}-containing POM systems.

Herein, we report on the reactivity of Pb^{II} ions with monolacunary Keggin-type 11-tungstosilicate and -germanate polyanions.

2 Experimental methods

2.1 Synthesis of $K_6[Pb(\alpha\text{-}SiW_{11}O_{39})]\ (Pb(NO_3)_2)_{0.2}\cdot 36H_2O\cdot$ **(K-1)**

$K_8[\alpha\text{-}SiW_{11}O_{39}]\cdot 13H_2O$ (0.303 g, 0.094 mmol) was dissolved with heating (~80 ˚C) in 10 mL of 0.5 M KNO_3. To this solution, $Pb(NO_3)_2$ (0.05 g, 0.151 mmol) was added, and the resulting dispersion was heated in a water bath at 80˚C for 90 min. After the reaction, the solution was allowed to cool to room temperature and white needle-like crystals formed along with an amorphous precipitate. The cooled mixture was filtered, and the clear mother liquor was left for slow evaporation at room temperature. Colorless needle-shaped crystals (Fig. S1) of **K-1** were collected after 2 days and washed with cold water. Yield: 0.18 g (50%, based on W). IR data (KBr pellet) (in cm^{-1}): 1619 (s), 1389 (s), 997 (m), 951 (w), 904 (sh), 796 (s), 691(sh), 524 (w), 477 (w). Elemental analysis, calcd (found) for **K-1**: W, 52.6 (52.5); Pb, 6.4 (6.2); K, 6.1 (6.5); Si, 0.7 (0.8).

2.2 Synthesis of $K_6[Pb(\alpha\text{-}GeW_{11}O_{39})]\cdot(Pb(NO_3)_2)_{0.2}\cdot 39H_2O$ **(K-2)**

$K_6Na_2[\alpha\text{-}GeW_{11}O_{39}]\cdot 13H_2O$ (0.304 g, 0.094 mmol) was dissolved with heating (~80 ˚C) in 10 mL of 0.5 M KNO_3. To this solution, $Pb(NO_3)_2$ (0.05 g, 0.151 mmol) was added, and the resulting dispersion was heated in a water bath at 80˚C for 90 min. After the reaction, the solution was allowed to cool to room temperature and white needle-like crystals formed along with an amorphous precipitate. The cooled mixture was filtered, and the clear mother liquor was left for slow evaporation at room temperature. Colorless needle-shaped crystals (Fig. S1) of **K-2** were collected after 2 days and washed with cold water. Yield: 0.20 g (54%, based on W). IR data (KBr pellet) (in cm^{-1}): 1620 (s), 1386 (s), 951 (s), 879 (m), 809 (sh), 714 (w), 518 (m), 454 (m). Elemental analysis, calcd (found) for **K-2**: W, 51.3 (51.5); Pb, 6.3 (5.7); K, 5.9 (6.4); Ge, 1.8 (1.6).

General methods and materials

All reagents were purchased from commercial sources and used without further purification. The monolacunary POM precursor salts $K_8[\alpha\text{-}SiW_{11}O_{39}]\cdot 13H_2O$ (**K-SiW$_{11}$**) and $K_6Na_2[\alpha\text{-}GeW_{11}O_{39}]\cdot 13H_2O$ (**KNa-GeW$_{11}$**) were synthesized according to the published procedures [23, 24], and characterized by IR and NMR spectroscopy. Fourier-transform infrared spectroscopy (FT-IR) was performed on KBr pellets using a SHIMADZU FT-IR spectrophotometer in the range of 4000-400 cm^{-1}. The relative peak intensities are denoted as w = weak, m = medium, s = strong, and sh = shoulder. Room-temperature ^{183}W NMR spectra were recorded on a JEOL ECX 400 MHz spectrometer in aqueous solution, using D_2O as locking solvent. The ^{183}W resonance frequency was 16.687 MHz, and all chemical shifts were referenced to a 1 M Na_2WO_4 solution. Thermogravimetric analysis (TGA) was carried out on a TA Instruments Q600 analyzer under a nitrogen atmosphere by heating the sample from room temperature to 600 °C at a rate of 5 °C min^{-1}. Elemental analysis for Pb, W, Si and Ge were conducted by Technische Universität Hamburg, Zentrallabor Chemische Analytik, Eißendorfer Straße 38, Gebäude O, 21073 Hamburg. Powder X-ray diffraction (PXRD) data were collected on a Rigaku Miniflex 600 diffractometer equipped with Cu Kα radiation (λ = 1.541838 Å). The instrument was operated at 40 kV and 15 mA, and patterns were recorded over the 2θ range of 3–80° using a step size of 0.01° and a scan rate of 2° min^{-1}.

X-ray crystallography. Single-crystal X-ray diffraction data were collected at 100 K on a Rigaku XtaLAB Synergy diffractometer equipped with a Dualflex source and HyPix detector system, using kappa geometry and Cu Kα radiation (λ = 1.54184 Å. Suitable crystals were mounted on Hampton cryoloops with Paratone-N oil prior to data collection. Data collection, reduction, and initial processing were carried out using CrysAlisPro [25]. Absorption effects were corrected empirically using the ABSPACK program [26]. The structure was solved using Olex2 [27], and refined against F^2 by full-matrix least-squares methods with the SHELX program package [28,29]. For structures containing highly disordered solvent molecules, the SQUEEZE routine in PLATON was applied where necessary [30]. The crystallographic and refinement parameters are summarized in Table 1. CIF files are available free of charge from The Cambridge Crystallographic Data Centre (2571187 for **K-1**, 2571188 for **K-2**).

Table 1. Single crystal data and structure refinement parameters for **K-1** and **K-2**.

Compound	**K-1**	**K-2**

Under Review

Empirical Formula[a]	$Si_2K_{10}O_{96}Pb_2W_{22}$ ($SiH_{72}K_6N_{0.4}O_{76.2}Pb_{1.2}W_{11}$)	$Ge_2K_9O_{86}Pb_2W_{22}$ ($GeH_{78}K_6N_{0.4}O_{79.2}Pb_{1.2}W_{11}$)
Formula weight g mol^{-1}	6442.06	6332.00
Crystal system	Orthorhombic	Orthorhombic
Space group	$Pna2_1$	$Pna2_1$
a (Å)	17.4918 (8)	17.5779 (9)
b (Å)	20.4943 (7)	20.5060 (8)
c (Å)	13.6554 (5)	13.6309 (6)
α (deg)	90	90
β (deg)	90	90
γ (deg)	90	90
Volume, $Å^3$	4895.2 (3)	4913.3(4)
Z	2	2
D_{calc}, g/cm^3	4.371	4.280
Crystal size, mm × mm × mm	0.16 × 0.1 × 0.07	0.18 × 0.09 × 0.06
Absorption coefficient, mm^{-1}	57.907	57.612
F(000)	5556.0	5430.0
2θ range for data collection, deg	6.644 to 163.218	6.624 to 163.34
Index ranges	$-22 \le h \le 22$ $-26 \le k \le 26$ $-15 \le l \le 17$	$-21 \le h \le 18$ $-26 \le k \le 26$ $-17 \le l \le 17$
Reflections collected	78213	135456
Independent reflections	10853	10893
R(int)	0.0857	0.0917
Data/restraints/parameters	10853/391/355	10893/1/354
Goodness-of-fit on F^2	1.065	1.083
R_1,[b] wR_2[c] ($I > 2\sigma(I)$)	$R_1 = 0.0636$, $wR_2 = 0.1503$	$R_1 = 0.0532$, $wR_2 = 0.1478$
R_1,[b] wR_2[c] (all data)	$R_1 = 0.0690$, $wR_2 = 0.1567$	$R_1 = 0.0580$, $wR_2 = 0.1583$
Largest diff peak and hole, e $Å^{-3}$	5.86 and -3.74	3.53 and -2.76

[a] The entries in the parentheses represent the actual formula units as determined from elemental analysis on bulk samples. [b] $R_1 = \sum||F_o| - |F_c||/\sum|F_o|$. [c] $wR_2 = [\sum w (F_o^2 - F_c^2)^2 / \sum w (F_o^2)^2]^{1/2}$

3 Results and discussion

3.1 Synthesis and Structure

Reaction between the nitrate salt of Pb^{II} and the monolacunary Keggin precursors $K_8[\alpha\text{-}SiW_{11}O_{39}]\cdot 13H_2O$ or $K_6Na_2[\alpha\text{-}GeW_{11}O_{39}]\cdot 13H_2O$ in a 0.5 M KNO_3 solution resulted in the formation of the Pb^{II}-containing polyanions $[Pb^{II}(\alpha\text{-}XW_{11}O_{39})]^{6-}$ (X = Si, **1**; Ge, **2**), see Fig. 1 and S6. In **1** and **2** the Pb^{II} guest ion occupies the lacunary site of the respective Keggin host and single-crystal X-ray diffraction (XRD) revealed the four equatorial Pb-O bonds range from 2.391 to 2.492 Å for **1** and from 2.415 to 2.500 Å for **2**. The potassium salts of polyanions **1** and **2** crystallize in the orthorhombic system, space group $Pna2_1$ and hence both salts are isomorphous. In the solid state both polyanions **1** and **2** exhibit an infinite one-dimensional arrangement, with the Pb^{II} ion of one polyanion being connected to four bridging W-O(W) oxygens of the neighboring polyanion, see Fig. 2. Hence the Pb^{II} ions in both **1** and **2** are 8-coordinated resulting in a square-antiprismatic geometry (Fig. 3).

Just Accepted

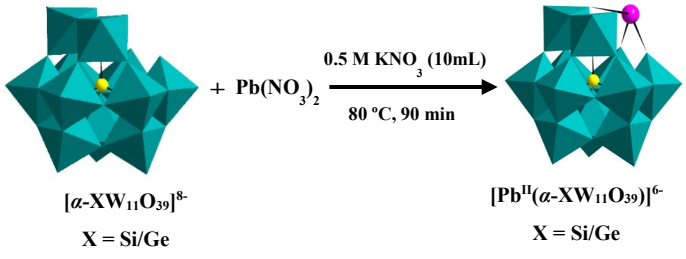


Figure 1. Scheme showing the preparation of $[Pb^{II}(\alpha\text{-}XW_{11}O_{39})]^{6-}$ (X = Si, Ge). Color code: Pb, pink; X, yellow; WO_6 octahedra, cyan.

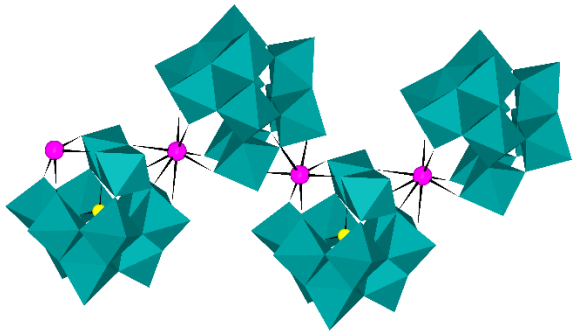


Figure 2. Combined polyhedral/ball-and-stick representation of the one-dimensional arrangement of polyanions **1** and **2** in the solid state. Color code: Pb, pink; X, yellow; WO_6 octahedra, cyan.

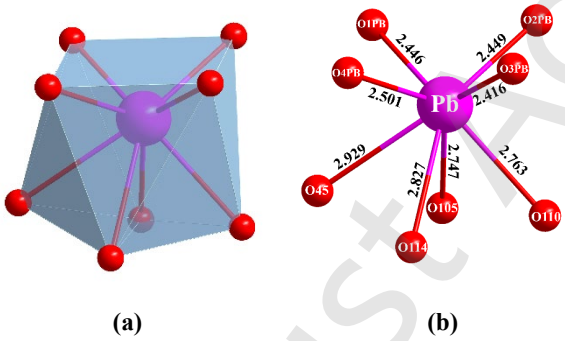


Figure 3. (a) Coordination polyhedron of Pb(II) in **K-1** and **K-2**, each formed by eight oxygen atoms, displaying a distorted square-antiprismatic geometry; (b) Pb-O coordination environment with the corresponding bond distances (Å) for **K-2** as a representative. Color code: PbO_8 polyhedron, pale blue; Pb, pink; O, red.

Due to the isostructural nature of **1** and **2**, only polyanion **2** is described here in detail, as a representative of both polyanions. Considering that the Pb^{II} ion is significantly larger than W^{VI} (for the same coordination number) the former does not fit fully into the Keggin lacunary site and is displaced outward (see Fig. S6). This is also reflected in the long Pb···W separations of ca 3.8 Å. Usually W···W separations in POMs are around 3.3 Å for edge-shared octahedra and 3.6 Å for corner-shared octahedra. The exposed position of Pb in **2** allows the lead ion to coordinate to neighboring polyanions via four Pb-O(W) bonds, resulting in a 1D-chain with the polyanions alternatingly located up and down. The oxidation state of the Pb atom is confirmed to be +2 by bond valence sum calculations (BVS), see Table S1. All tungsten atoms in **2** have the expected distorted octahedral coordination geometry with the W^{VI} atoms being displaced towards the terminal oxo ligand. The +6 oxidation state was confirmed by BVS calculations [31], see Table S2 and Table S3. The bonding and structural details are pretty much analogous for polyanion **1**, except that the Ge-O (ca 1.7 Å) vs Si-O (ca 1.6 Å) bond lengths differ by about 0.1 Å. The Pb(II) substituted **K-SiW$_{11}$** and **K-GeW$_{11}$** compounds illustrate the dual coordination role of Pb(II) as both lacunary site substituent and an inter POM linker. The resulting PbO_8 coordination (Fig. 3) and its preservation in both Si- and Ge-cantered derivatives highlights the flexible and robust nature of this Pb-directed assembly.

The present Si(IV)- and Ge(IV)- containing compounds extends the structural chemistry of Pb(II)-incorporated monolacunary Keggin tungstates to group-14-heteroatoms, complementing the previously reported group-13 Ga(III) and group-15 P(V) derivatives. In the group-1f3 Ga(III) compound, $[GaPbW_{11}O_{39}]^{7-}$, Pb(II) is coordinated to four oxygen atoms of lacunary GaW_{11} unit with a pyramidal arrangement [11]. In contrast, the group-15 phosphotungstate derivative $[PW_{11}O_{39}Pb]^{5-}$ was reported as discrete 1:1 species with square pyramidal Pb(II) environment [20]. The present Si(IV)- and Ge(IV)- based compounds extends this family to group-14-heteroatom (monolacunary species) and are distinguished by eight coordinate Pb(II) environment.

The IR spectrum of **K-1** (Fig. S2) exhibits the expected features such as a band at 997 cm^{-1} which is assigned to the Si-O stretching vibrations, associated with the SiO_4 hetero group in the structure. The intense band at 950 cm^{-1} arises from the stretching vibration of the terminal W=O bonds. The bands at 904 cm^{-1} and at 524 and 477 cm^{-1} are associated with the stretching and bending vibrations of the W-O(W) bonds, respectively. Analogously, the IR spectrum of **K-2** (Fig. S3) shows a band at 809 cm^{-1} which is assigned to the Ge-O stretching vibrations associated with the GeO_4 hetero group in the structure. The intense band at 951 cm^{-1} arises from the stretching vibration of the terminal W=O bonds, whereas the bands at 879 cm^{-1} and at 518 and 454 cm^{-1} are associated with the stretching and bending vibrations of the W-O(W) bonds, respectively [32,33]. In both the cases the low frequency region (400-600cm^{-1}) likely contains contributions from both Pb-O and W-O-W vibrations. Additionally, the absorption band observed at 1389 cm^{-1} for **K-1** and 1386 cm^{-1} for **K-2** is attributed to the symmetric stretching vibration of nitrate ions, possibly arising from the co-crystallized lead(II)nitrate present in both the compounds.

Just Accepted

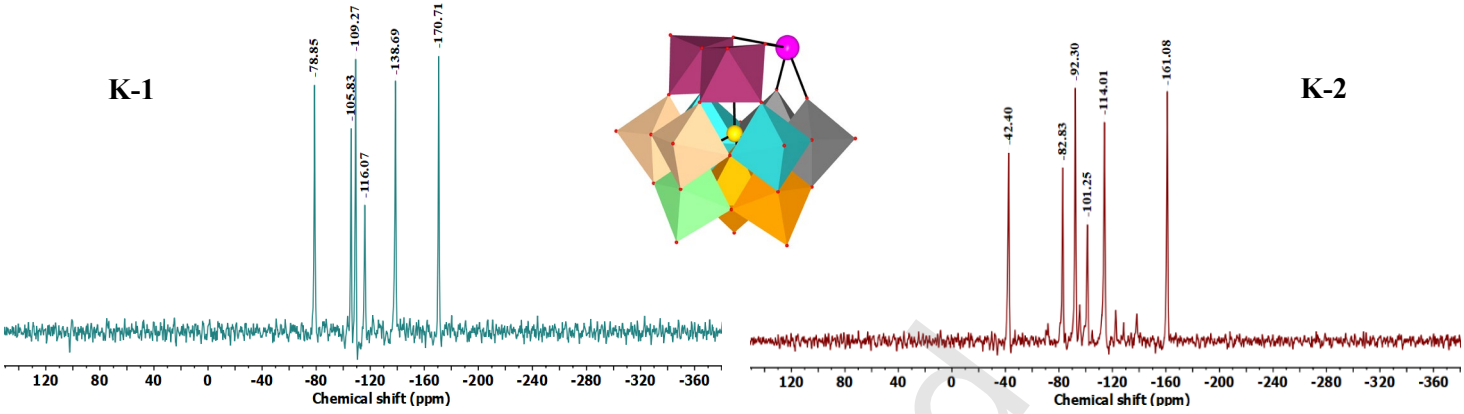


Figure 4. ^{183}W NMR spectra of **K-1** (left) and **K-2** (right) recorded in 2 M sodium acetate buffer (pH 4) at room temperature. The polyhedral structure representing both polyanions indicates the magnetically equivalent W atoms in the same color.

Table 2. Summary of ^{183}W NMR chemical shifts for **K-1**, **K-2**, **K-SiW$_{11}$**, and **KNa-GeW$_{11}$**. The relative intensities are shown in brackets.

Compound	Chemical Shift (ppm)
K-1[a]	-78.8(2), -105.8(2), -109.2(2), -116.0(1), -138.7(2), -170.7(2)
K-2[a]	-42.4(2), -82.8(2), -92.3(2), -101.2(1), -114.0(2), -161.1(2)
K-SiW$_{11}$[b]	-95.8(2), -116.4(2), -118.8(1), -123.8(2), -139.8(2), -172.9(2)
KNa-GeW$_{11}$[b]	-81.5(2), -107.7(2), -116.4(1), -123.6(2), -145.1(2), -163.6(2)

[a] Recorded using 0.8 g of sample in 2 M sodium acetate buffer (pH 4).
[b] Recorded using 0.8 g of sample in H_2O.

The ^{183}W NMR spectra of compounds **K-1** and **K-2** were recorded in 2 M sodium acetate buffer (pH 4) at room temperature (Fig. 4). For **K-1** the six expected resonances were observed at -78.8, -105.8, -109.2, -116.0, -138.7, and -170.7 ppm, respectively, with intensity ratios of 2:2:2:1:2:2, indicating that the unique W atom resonates at -116.0 ppm. For **K-2** the situation is analogous, the six resonances being observed at -42.3, -82.8, -92.3, -101.2, -114.0, and -161.1 ppm, respectively, with the peak of the unique W atom located at -101.2 ppm. The observed chemical shifts of **1** and **2** are summarized in Table 2, together with those of the lacunary precursors **K-SiW$_{11}$** and **KNa-GeW$_{11}$** recorded in H_2O.

The thermogravimetric curves of freshly prepared **K-1** and **K-2** (see Fig. S4) indicate an initial two-step weight loss up to around 208 °C for **K-1** and ca. 223 °C for **K-2**, corresponding to the loss of lattice water molecules, in which the initial dehydration could be due to the removal of relatively weakly bound lattice water molecules followed by the step removal of more strongly bound water molecules. (calculated ~5.2% for **K-1** and ~5.7% for **K-2**. The dehydration observed by TGA corresponds to lower water content (for both **K-1** and **K-2**) than the calculated formulas by elemental analysis, likely because part of weakly bound lattice water was lost before TGA measurement during drying, storage or sample handling.

Powder XRD measurements for **K-1** and **K-2** (Fig. S5) were performed to check the crystalline phases of the prepared samples. The primary peaks in the experimental powder XRD patterns (at room temperature) show reasonable agreement with simulated patterns calculated from single-crystal XRD data collected at 100 K, with the differences in the relative peak intensities which may be associated with the preferred orientation of the crystallites on the surface of the powder sample.

Conclusions

We have synthesized and structurally characterized two lead(II)-containing heteropoly-11-tungstates of the Keggin type, [Pb^{II}(α-XW$_{11}$O$_{39}$)]$^{6-}$ (X = Si, **1**; Ge, **2**). The Pb^{II} ion occupies the lacunary site of the monovacant Keggin ions, although it cannot fully enter due to its large size. This fact favours the interaction with neighboring polyanions in the solid state, with each Pb^{II} ion coordinating to four oxygens of a neighboring polyanion, resulting in coordination number 8, and the formation of a one-dimensional chain. The two products **K-1** and **K-2** were characterized in the solid state by FTIR spectroscopy, thermogravimetric analysis, powder-XRD and elemental analysis, and in solution by ^{183}W NMR spectroscopy, indicating the expected spectrum of 6 signals with intensity ratios 2:2:2:1:2:2,

Just Accepted

reflecting the *Cs* point group symmetry of **1** and **2**. In the future, we aim at isolating and characterizing other POMs containing Pb^{II} or Pb^{IV} as guest ion.

Electronic Supplementary Material: Supplementary material (FTIR spectra, thermograms, bond lengths and powder XRD of **K-1** and **K-2**) is available in the online version of this article at https://doi.org/10.26599/POM.2026.9140176.

Data availability

All data needed to support the conclusions in the paper are presented in the manuscript and/or the Electronic Supplementary Material. Additional data related to this paper may be requested from the corresponding author upon request.

2571187 and 2571188 contain the supplementary crystallographic data for this paper. These data can be obtained free of charge via www.ccdc.cam.ac.uk/structures/, or by emailing data_request@ccdc.cam.ac.uk, or by contacting The Cambridge Crystallographic Data Centre, 12 Union Road, Cambridge CB2 1EZ, UK; fax: +44 1223 336033

Acknowledgements

U.K. thanks the German Research Council (DFG, KO-2288/29-1, KO-2288/31-1, and KO-2288/33-1) and Constructor University for support. The polyanion structures in Figures 1 and 2 were generated with Diamond, version 3.2 (Crystal Impact GbR).

Dedication

This paper is dedicated to the memory of Ulrich Kortz, whose contributions to this field continue to inspire us.

Declaration of competing interest

There are no conflicts to declare. The author Ulrich Kortz was a guest editor for this special issue and an advisory board member of this journal, but he was not involved in the peer-review or decision of this article.

Author contribution statement

L. K: Data curation, validation, writing manuscript. N. N.: Data curation, validation. A. S.: Data curation, validation. A. R.: Data curation, validation. A. A. G.: Data curation. U. K.: Project administration, funding acquisition, supervision. All the authors have approved the final manuscript.

Use of AI statement

None.

4 References

[1] Pope, M. T. *Heteropoly and Isopoly Oxometalates*; Springer-Verlag: Berlin, **1983**.

[2] Liu, L.-L.; Wang, L.; Xiao, X.-Y.; Yang, P.; Zhao, J.; Kortz, U. Structural overview and evolution paths of lacunary polyoxometalates. *Coord. Chem. Rev.* **2024**, *506*, 215687.

[3] Hussain, F.; Kortz, U.; Clark, R. J. The Bis-Phenyltin-Substituted, Lone-Pair-Containing Tungstoarsenate $[(C_6H_5Sn)_2As_2W_{19}O_{67}(H_2O)]^{8-}$. *Inorg. Chem.* **2004**, *43*, 3237-3241.

[4] Kortz, U.; Hussain, F.; Reicke, M. The Ball-Shaped Heteropolytungstates $[\{Sn(CH_3)_2(H_2O)\}_{24}\{Sn(CH_3)_2\}_{12}(A\text{-}XW_9O_{34})_{12}]^{36-}$. *Angew. Chem. Int. Ed.* **2005**, *44*, 3773-3777.

[5] Hussain, F.; Dickman, M. H.; Kortz, U.; Keita, B.; Nadjo, L.; Khitrov, G. A.; Marshall, A. G. Trimeric, Cyclic Dimethyltin-Containing Tungstophosphate $[\{(Sn(CH_3)_2)(Sn(CH_3)_2O)(A\text{-}PW_9O_{34})\}_3]^{21-}$. *J. Cluster Sci.* **2007**, *18*, 173-191.

[6] Keita, B.; de Oliveira, P.; Nadjo, L.; Kortz, U. The Ball-Shaped Heteropolytungstates $[\{Sn(CH_3)_2(H_2O)\}_{24}\{Sn(CH_3)_2\}_{12}(A\text{-}XW_9O_{34})_{12}]^{36-}$ (X = P, As): Stability, Redox, and Electrocatalytic Properties in Aqueous Media. *Chem. Eur. J.* **2007**, *13*, 5480-5491.

[7] Piedra-Garza, L. F.; Barsukova-Stuckart, M.; Bassil, B. S.; Al-Oweini, R.; Kortz, U. Diethyltin-Containing Tungstoarsenate(V), $[\{Sn(C_2H_5)_2\}_3(H_2O)_6(A\text{-}\alpha\text{-}As^{V}W_9O_{34})]^{3-}$. *J. Cluster Sci.* **2012**, *23*, 939-951.

[8] Shimoni-Livny, L.; Glusker, J. P.; Bock, C. W. Lone Pair Functionality in Divalent Lead Compounds. *Inorg. Chem.* **1998**, *37*, 1853-1867.

[9] Shannon, R. D. Revised Effective Ionic Radii and Systematic Studies of Interatomic Distances in Halides and Chalcogenides. *Acta Crystallogr., Sect. A* **1976**, *32*, 751-767.

[10] Yang, P.; Ma, T.; Lang, Z..; Misirlic-Dencic, S.; Isakovic, A. M.; Bényei, A.; Čolović, M. B.; Markovic, I.; Krstić, D. Z.; Poblet, J. M.; Lin, Z.; Kortz, U. Tetravalent Metal Ion Guests In Polyoxopalladate Chemistry: Synthesis and Anticancer Activity of $[MO_8Pd_{12}(PO_4)_8]^{12-}$ (M = Sn(IV), Pb(IV)). *Inorg. Chem.* **2019**, *58*, 11294-11299.

[11] Tourné, G. F.; Tourné, C. M.; Schouten, A. Plomb(II)-undecatungstogallate(III)(7-) de Potassium Hexadécahydraté. *Acta Crystallogr., Sect. B* **1982**, *38*, 1418-1422.

[12] Brevard, C.; Schimpf, R.; Tourné, G. F.; Tourné, C. M. Tungsten-183 NMR: A Complete and Unequivocal Assignment of the Tungsten-Tungsten Connectivities in Heteropolytungstates via Two-Dimensional ^{183}W NMR Techniques. *J. Am. Chem. Soc.* **1983**, *105*, 7059-7063.

[13] Radkov, E. V.; Beer, R. H. A comprehensive series of Group 14 derivatives of the plenary mixed-metal polyoxometalate $[PNbW_{11}O_{40}]^{4-}$. *Inorg. Chim. Acta* **2000**, *297*, 191-198.

[14] Yoshida, A.; Nakagawa, Y.; Uehara, K.; Hikichi, S.; Mizuno, N. Inorganic Cryptand: Size-Selective Strong Metallic Cation Encapsulation by a Disilicoicosatungstate (Si_2W_{20}) Polyoxometalate. *Angew. Chem. Int. Ed.* **2009**, *48*, 7055-7058.

[15] Udalova, L. I.; Adonin, S. A.; Abramov, P. A.; Korolkov, I. V.; Yunoshev, A. S.; Plyusnin, P. E.; Sokolov, M. N. Complexes of non-lacunary Keggin- and Dawson-type polyoxometalates with Pb(II): Formation of 1D coordination polymers with different bonding modes. *New J. Chem.* **2016**, *40*, 9981-9985.

[16] Han, Z.; Xin, X.; Zheng, R.; Yu, H. Influence of Pb element on the catalytic properties of $\{P_4Mo_6\}$-polyoxometalate for redox reactions. *Dalton Trans.* **2018**, *47*, 3356-3365.

[17] Bushmeleva, E. P.; Kompankov, N. B.; Shiriyazdanov, R. R.; Karimova, A. R.; Abramov, P. A.; Sokolov, M. N. Chemistry of $[PW_{11}NbO_{40}]^{4-}$: Structural rearrangement and metal coordination. *Inorg. Chem. Commun.* **2018**, *98*, 180-183.

[18] Pang, T.; Zhou, Z.; Li, D.; Liu, H.; Zhang, Z.; Qi, L.; Song, C.-Y.; Gao, G.-G.; Lv, Y. Crystal Structure and Reversible Photochromism of Pb(II)-N,N-Dimethylformamide-Modified

Just Accepted

Keggin-Type Polyoxometalates. *Cryst. Res. Technol.* **2019**, *54*, 1900153.

[19] Lin, J.; Zhu, L.; Yue, Z.; Yang, C.; Liu, W.; Albrecht-Schmitt, T. E.; Wang, J.-Q.; Wang, S. [Ln_6O_8] Cluster-Encapsulating Polyplumbites as New Polyoxometalate Members and Record Inorganic Anion-Exchange Materials for ReO_4^- Sequestration. *Adv. Sci.* **2019**, *6*, 1900381.

[20] Mukhacheva, A. A.; Asanova, T.; Ryzhikov, M. R.; Sukhikh, T. S.; Kompankov, N. B.; Yanshole, V. V.; Berezin, A. S.; Gushchin, A. L.; Abramov, P. A.; Sokolov, M. N. Keggin-type polyoxometalate 1:1 complexes of Pb(II) and Bi(III): Experimental, theoretical, and luminescence studies. *Dalton Trans.* **2021**, *50*, 6913-6922.

[21] Zhang, J.; Wang, X.; Wang, G.; Feng, Y.; Zhang, C.; Pang, T.; Gao, G.; Fan, L.; Liu, H. Ultrasensitive photochromism and impedance dual response to weak visible light by solvated Pb(II)-modified polyoxomolybdate. *Chin. Chem. Lett.* **2023**, *34*, 107231.

[22] Ambar, T.; Kar, A.; Baranov, M.; Leffler, N.; Neyman, A.; Weinstock, I. A. Polyoxometalate Ligation of PbS Nanocrystals. *Inorg. Chem.* **2025**, *64*, 8952-8957.

[23] Tézé, A.; Hervé, G. alpha-, beta-, and gamma-Dodecatungstosilicic acids: Isomers and Related Lacunary Compounds. in *Inorganic Syntheses*; Ginsberg, A. P., Ed.; John Wiley & Sons, Inc., **1990**; Vol. *27*, pp 89.

[24] Haraguchi, N.; Okaue, Y.; Isobe, T.; Matsuda, Y. Stabilization of Tetravalent Cerium Upon Coordination of Unsaturated Heteropolytungstate Anions. *Inorg. Chem.* **1994**, *33*, 1015-1020.

[25] Rigaku. CrysAlis PRO Software System, version 1.171.43.97a; Rigaku Oxford Diffraction, **2023**.

[26] Rigaku. ABSPACK, SCALE empirical absorption correction, CrysAlis Pro software package; Rigaku Oxford Diffraction, **2023**.

[27] Dolomanov, O. V.; Bourhis, L. J.; Gildea, R. J.; Howard, J. A. K.; Puschmann, H. OLEX2: a complete structure solution, refinement, and analysis program. *J. Appl. Crystallogr.* **2009**, *42*, 339-341.

[28] Sheldrick, G. M. SHELXT-Integrated space-group and crystal-structure determination. *Acta Crystallogr., Sect. A* **2015**, *71*, 3-8.

[29] Sheldrick, G. M. Crystal structure refinement with SHELXL. *Acta Crystallogr., Sect. C* **2015**, *71*, 3-8.

[30] Spek, A. L. PLATON SQUEEZE: a tool for the calculation of the disordered solvent contribution to the calculated structure factors. *Acta Crystallogr., Sect. C* **2015**, *71*, 9-18.

[31] Brown, I. D.; Altermatt, D. "Bond-Valence Parameters Obtained from a Systematic Analysis of the Inorganic Crystal Structure Database." *Acta Crystallogr., Sect. B* **1985**, *41*, 244-247.

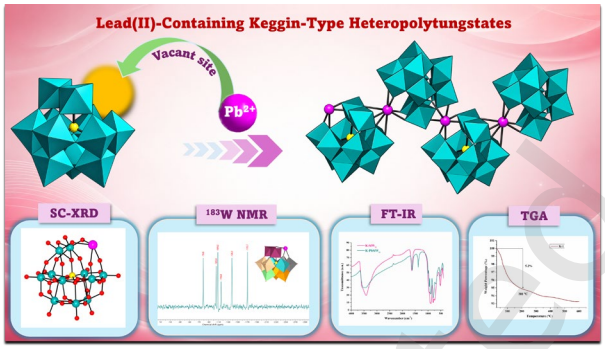
[32] Rocchiccioli-Deltcheff, C.; Fournier, M.; Franck, R.; Thouvenot, R. Vibrational Investigations of Polyoxometalates. 2. Evidence for Anion-Anion Interactions In Molybdenum(VI) and Tungsten(VI) Compounds Related to the Keggin structure. *Inorg. Chem.* **1983**, *22*, 207-216.

[33] Thouvenot, R.; Fournier, M.; Franck, R.; Rocchiccioli-Deltcheff, C. Vibrational Investigations of Polyoxometalates. 3. Isomerism in Molybdenum(VI) and Tungsten(VI) Compounds Related to the Keggin Structure. *Inorg. Chem.* **1984**, *23*, 598-605.

Just Accepted

Table of Contents artwork

Two lead(II)-substituted Keggin-type polyoxometalates, **$PbSiW_{11}$** and **$PbGeW_{11}$**, have been synthesized and structurally characterized in the solid state by XRD, FT-IR, TGA, and elemental analysis, and in solution by ^{183}W NMR. In the solid state the polyanions assemble into an infinite one-dimensional chain via Pb-O(W) coordination to a neighboring polyanion.



Just Accepted